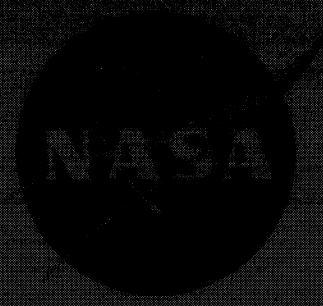

FINAL REPORT
RESEARCH ON THE PROPERTIES OF BINARY LIQUID METAL SYSTEMS WITH LITHIUM AS ONE COMPONENT

THE ELECTRICAL RESISTIVITY OF LIQUID LITHIUM SATURATED WITH CESIUM

by

F.F. Felber Jr., S.M. Kapetner, and K.A. Helgeson

FEBRUARY 13, 1970

CONTRACT NUMBER NAS7-668

Prepared for

JET PROPULSION LABORATORY, NASA PASADENA OFFICE
4800 OAK GROVE DRIVE PASADENA, CALIFORNIA 91103

David G. Elliot, Project Manager

Pratt & Whitney Aircraft
DIVISION OF UNITED AIRCRAFT CORPORATION

Pratt & Whitney Aircraft DIVISION OF UNITED AIRCRAFT CORPORATION

In reply please refer to:
FFF:REF:cw – Bldg. 450, Middletown

15 April 1970

To: National Aeronautics and Space Administration
Chief, Nuclear Systems and Space Power Division
Code RN
Washington, D.C. 20546

Subject: Final Report; Research on Properties of Binary Liquid Metal Systems With Lithium as One Component. The Electrical Resistivity of Liquid Lithium Saturated With Cesium, PWA-3877

Reference: Contract Number NAS7-658

Enclosure: Copy of Subject Report

A copy of the subject report is submitted herewith in compliance with the requirements of Article II, Paragraph D of the referenced contract as modified by Amendment No. 3 dated 27 August 1969. One hundred and twenty five (125) copies (specified by Contract) of this final report are being distributed in accordance with the distribution list supplied by the contracting officer and shown at the back of the report.

UNITED AIRCRAFT CORPORATION
Pratt & Whitney Aircraft Division

Frank F. Felber, Jr.

Frank F. Felber, Jr.
Program Manager

cc: Dr. D. G. Elliot, Technical Manager (1 copy)
Jet Propulsion Laboratory
NASA Pasadena Office
4800 Oak Grove Drive
Pasadena, California 91103

Mr. Edward Lonning, Contracting Officer's Representative (3 copies)
Jet Propulsion Laboratory
NASA Pasadena Office
4800 Oak Grove Drive
Pasadena, California 91103

FINAL REPORT
RESEARCH ON THE PROPERTIES OF BINARY LIQUID METAL SYSTEMS WITH LITHIUM AS ONE COMPONENT

THE ELECTRICAL RESISTIVITY OF LIQUID LITHIUM SATURATED WITH CESIUM

PWA-3877

by
F. F. Felber, Jr., S. M. Kapelner, and K. A. Helgeson

February 13, 1970

Contract Number NAS7-658

Prepared for
JET PROPULSION LABORATORY, NASA PASADENA OFFICE
4800 OAK GROVE DRIVE PASADENA, CALIFORNIA 91103
David G. Elliot, Project Manager

Pratt & Whitney Aircraft DIVISION OF UNITED AIRCRAFT CORPORATION

ABSTRACT

The electrical resistivity of a saturated solution of cesium in liquid lithium has been measured in the temperature range from 770°C to 1100°C in a Haynes-25 alloy tube by a high precision potentiometric technique and compared with the electrical resistivity of the same sample of liquid lithium measured independently in the same container. Matthiessen's rule is obeyed to approximately 900°C confirming the low solubility of cesium in liquid lithium. The impurity atom resisitivity of cesium is less than one microhm-centimeter over this range, increasing to three microhm-centimeters at 1094°C.

The temperature dependence of the electrical resisivity of a saturated solution of cesium in lithium can be be expressed by the following equation:

$$\rho = 41.97 - 0.01585t + 2.271 \times 10^{-5} t^2$$

where ρ is the electrical resistivity in microhm-centimeters
and t is in degrees Centigrade.

The electrical resistivity of the liquid lithium as a function of temperature in the temperature range 365°C to 973°C is:

$$\rho = 21.48 + 0.03170t - 5.913 \times 10^{-6} t^2$$

These results indicate that cesium solubility would not significantly alter the generator efficiency with liquid lithium as the conducting fluid in a lithium-cesium, two-component, two-cycle liquid metal MHD generator.

TABLE OF CONTENTS

LIST OF ILLUSTRATIONS

LIST OF TABLES

I. SUMMARY

Liquid lithium accelerated by cesium vapor is presently being considered as the working fluid system in a two-component two-cycle liquid metal MHD energy conversion system. After separation of the vapor and liquid phases, the liquid lithium, which is saturated with cesium, decelerates in an MHD generator while producing electrical power. One of the factors influencing the efficiency of this system is the electrical resistivity of the working fluid. Since the resistivity of cesium is about four hundred percent greater than that of lithium at 1100°C, the effect of dissolved and entrapped cesium on the resistivity of lithium becomes an important factor in evaluating efficiency. For this reason, the electrical resistivity of liquid lithium was measured to 1100°C.

Because of corrosive reactions between liquid metals and insulating materials at high temperatures, liquid metal resistances were measured in parallel with a Haynes-25 alloy specimen container. Using a high precision potentiometric technique, the resistance of the empty metal specimen container was accurately measured in the temperature range between about 300°C and 1100°C. In this range, the container resistance R_C ($\mu\Omega$) as a function of t (°C) is given by:

$$R_C = 1009 + 0.3643t - 2.648 \times 10^{-4} t^2$$

The total parallel resistance of the liquid metal and the specimen container was then measured potentiometrically as a function of temperature with the specimen mounted in a Hastelloy-X heat sink 4-inches outside diameter by 2½-inches inside diameter by 15-inches long in a furnace comprised of three independently controlled 12-inch long heating elements. For each data point, the temperature measured by three Pt/Pt-10% Rh thermocouples welded to the specimen container was held constant to within ±0.5°C on the average, with a maximum spread of ±1°C. The liquid metal resistance was then determined from the equations for parallel resistances and the resistivity calculated from the accurately known diameter and length of the liquid metal column, corrected for thermal expansion of the Haynes-25 specimen container. The resistivity of lithium, ρ_{Li} ($\mu\Omega$ - cm), in the temperature range between 365°C and 973°C is given as a function of t (°C) by the equation:

$$\rho_{Li} = 21.48 + 0.03170t - 5.913 \times 10^{-6} t^2$$

The temperature dependence of the electrical resistivity of a saturated solution of cesium in lithium for the temperature range between 768°C and 1094°C is given by:

$$\rho_{Li\text{-}Cs} = 41.97 - 0.01585t + 2.271 \times 10^{-5} t^2$$

Matthiessen's rule is obeyed to about 900°C, confirming the low solubility of cesium in liquid lithium. The impurity atom resistivity of cesium is less than one microhm-centimeter over this range, increasing to about three microhm-centimeters at 1094°C. These results indicate that cesium solubility would not significantly alter the MHD generator efficiency using lithium-cesium as the working fluid system.

II. INTRODUCTION

In the two-component, two cycle liquid metal MHD energy conversion system concept, a liquid metal is circulated in a closed loop and accelerated by a liquid metal vapor from another loop. After separation of the vapor and liquid phases, the liquid metal decelerates while producing electric power in an MHD generator. The lithium-cesium system is presently being considered as the working fluid system at the Jet Propulsion Laboratory (References 1 and 2). Some of the reasons for choosing this combination are the following:

1. Liquid lithium has a low electrical resistivity and a low temperature coefficient of resistivity;
2. Liquid lithium posesses a high thermal conductivity, a wide liquid range, and a low vapor pressure, all desirable characteristics for a nuclear reactor coolant (References 3 and 4); and
3. Liquid cesium has a high vapor pressure and a low solubility in lithium (Reference 5).

In the proposed scheme, the cesium and lithium phases are separated, and the liquid lithium saturated with cesium flows through the MHD generator. Since the electrical resistivity of cesium is about four hundred percent greater than that of lithium at 1100°C (Reference 6), it is important to know the effect of dissolved and entrapped cesium on the resistivity of lithium in order to evaluate the efficiency of this two component system. For this reason, it was decided to measure the electrical resistivity of liquid lithium and a saturated solution of cesium in the same sample of liquid lithium to 1100°C.

III. PRINCIPLE OF THE METHOD

The high temperature electrical resistivity of alkali metals cannot be measured directly because of the corrosive reactions with electric insulating materials. Therefore, the method used was to measure the resistance of the liquid metal in parallel with a suitable metal container (Reference 3). The experimental arrangement is shown schematically in Figure 1.

The resistance of the tube with liquid metal is given by:

$$R_T = R_S \times \frac{E_T}{E_S} \quad (1)$$

where: R_T = total parallel resistance of the specimen container and the liquid metal ($\mu\Omega$)

R_S = resistance of the standard resistor ($\mu\Omega$)

E_T = algebraic sum of the forward and reverse potential drops across the specimen container taps

E_S = algebraic sum of the forward and reverse potential drops across the standard resistor

Potential drops are measured in both the forward and reverse directions in order to compensate for thermal effects.

The resistance of the liquid metal column can then be determined from:

$$R_{LM} = \frac{R_T \, R_C}{R_C - R_T} \quad (2)$$

where: R_{LM} = resistance of the liquid metal column ($\mu\Omega$)

R_T = has been defined in equation 1.

R_C = calibrated resistance of the empty specimen container

The liquid metal resistivity is obtained from the equation:

$$\rho_{LM} = R_{LM} \times \frac{A}{L} \quad (3)$$

where: ρ_{LM} = resistivity of the liquid metal ($\mu\Omega$-cm)

R_{LM} = has been defined in equation 2

A = cross-sectional area of the liquid metal column (cm^2)

L = length of well-defined liquid metal column (cm)

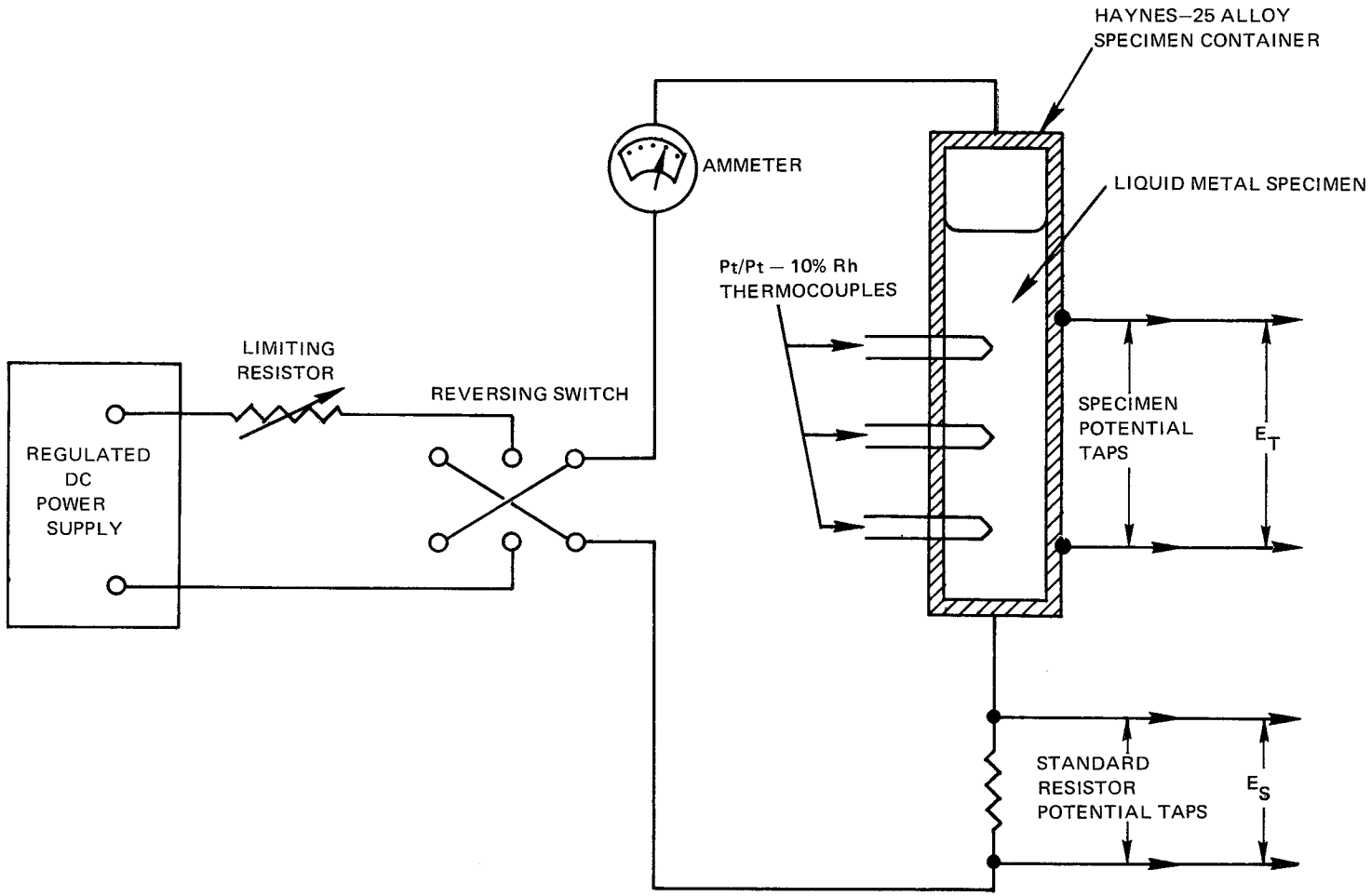

Figure 1 Schematic for Electrical Resistivity Measurements

The Haynes-25 specimen container will undergo significant thermal expansion between room temperature and the temperature of measurement. Therefore, it is necessary to correct the resistivity values for thermal expansion. The corrected value is given by:

$$\rho\text{corr} = \rho_{LM}(1 + \alpha\Delta T) \quad (4)$$

where: ρcorr = liquid metal resistivity corrected for thermal expansion of the specimen container

ρ_{LM} = resistivity of the liquid metal using room temperature dimensions in equation (3)

α = mean linear coefficient of thermal expansion between room temperature and the temperature of measurement (1/°C)

ΔT = difference between room temperature and the temperature of measurement (°C).

IV. DESCRIPTION OF APPARATUS

A. Specimen Container Design and Construction

The material chosen for the specimen container was Haynes-25 alloy because of its ability to meet the following design criteria:

1. Compatability with lithium and cesium to 1100°C,
2. Operation in an external air atmosphere to 1100°C,
3. High strength to withstand internal cesium vapor pressure to 250 psi at 1100°C,
4. Weldability in an inert atmosphere drybox, and
5. A parallel resistance which is high relative to that of the liquid metal it was to contain.

The specimen container tube was fabricated from a solid piece of bar stock. The inside diameter was electrochemically drilled to nearly the desired size and then honed to a constant bore. Desired wall thickness was obtained by turning the outside diameter on the centerline of the honed bore. The pumpout tube, which was used to evacuate the specimen container, was similarly fabricated, except that a constant bore and wall thickness was not required. Two specimen containers and one pumpout tube were fabricated. Figure 2 is a detailed drawing of the specimen container showing the finished dimensions of each one. Figure 3 illustrates the pumpout tube, and a drawing of the assembled specimen container is shown in Figure 4.

The scheme shown in Figure 4 could not be used for the lithium-cesium resistivity measurements because of severe bumping of the cesium at temperatures above 760°C, and because of the possibility of distilling the cesium into the cooler portions of the pumpout tube system. To eliminate this problem, it was necessary to immerse the entire specimen container in the heat zone. This was accomplished using the redesigned specimen container configuration shown in Figure 5. The tapered plug and screw arrangement shown in the right side of the figure served as a means of evacuating the specimen container after it had been filled with cesium. The procedure for doing this is described in another section of this report.

B. Heating System

The heating system, which is shown schematically in Figure 6, consisted of a modified 5-inch inside diameter clamshell furnace with three independently controlled 12-inch long heating zones. The three heating coils were made by hand-winding and cementing 0.057-inch diameter Kanthal A-1 resistance wire on spiral-grooved alumina cores 12-inches long by about 4¼-inches inside diameter. The cores were aligned axially to make a 36-inch long heat zone and then wrapped with enough fiber frax to provide a 2-inch thick insulating blanket. The original heating elements were removed, the insulated cores installed in their place, and the clamshell furnace closed. The power leads were passed through holes drilled in the metal furnace case. A short length of ceramic tubing slipped over the power leads served to insulate them electrically from the furnace case. The room temperature dc resistance of each winding was nine ohms. About 160 volts applied to each zone was sufficient to raise the temperature of the experiment to 1100°C in less than three hours.

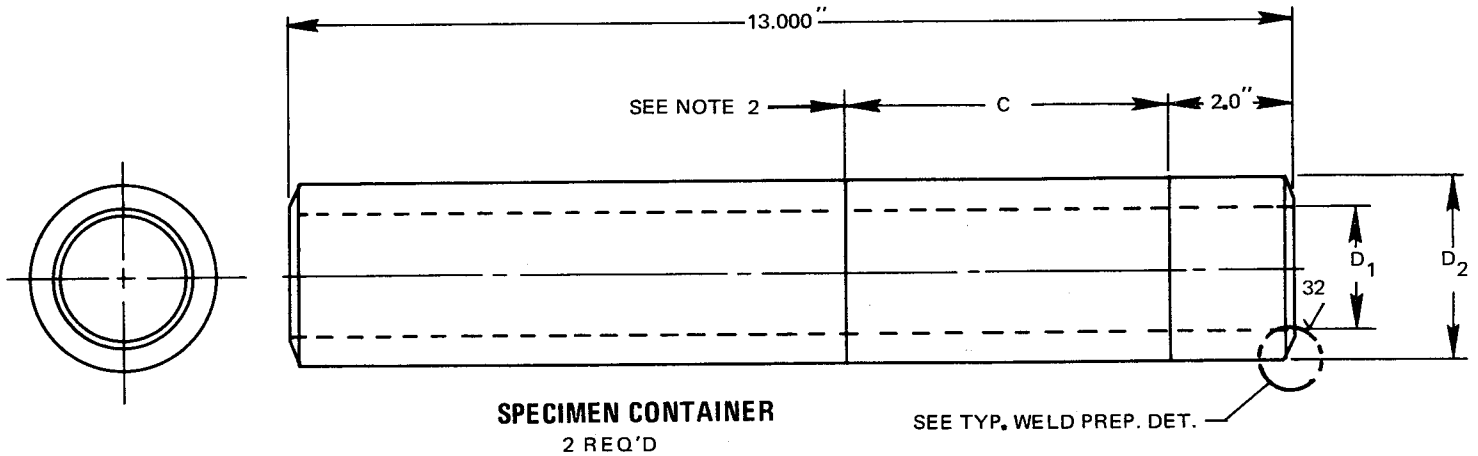

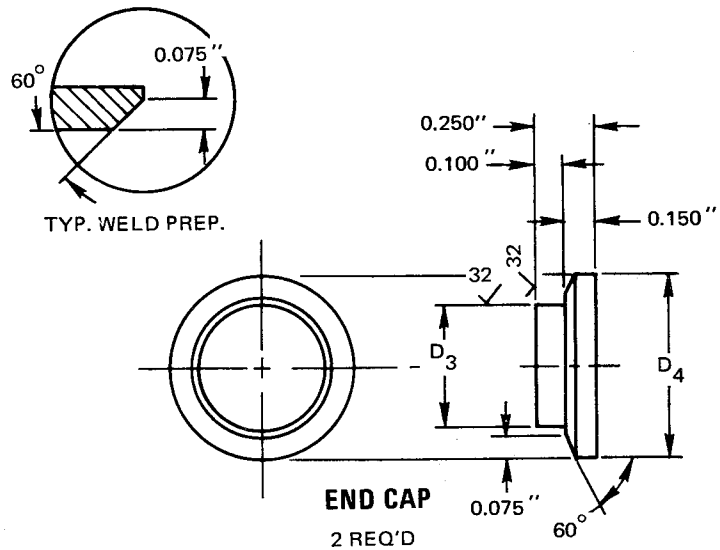

DIMENSIONS

SPEC CONT'R	C	D_1	D_2	D_3	D_4
A	4.000" ±0.002	0.5636" ±0.0005	0.7976" ±0.0005	0.5620" +0.000 -0.002	0.750" ±0.002
B	4.000" ±0.002	0.5885" ±0.0005	0.7785" ±0.0005	0.587" +0.000 -0.002	0.750" ±0.002

NOTES:

1 MAT'L TO BE HAYNES–25 MACHINED FROM SOLID BAR

2 SCRIBE 0.003" GROOVES ON OD OF TUBE AT LOCATIONS SHOWN

Figure 2 Specimen Container Detail

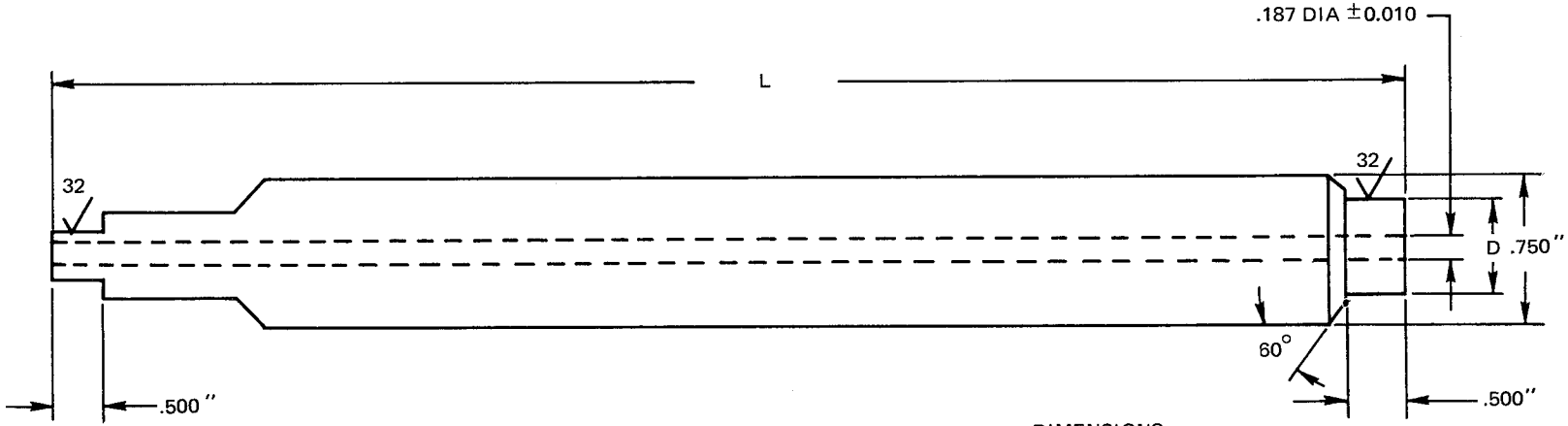

NOTES:

1 MAT'L TO BE HAYNES 25
MACHINED FROM SOLID BAR

2 ALL DIM'S ARE ±0.003" UNLESS
OTHERWISE SPECIFIED

DIMENSIONS

SPEC CONTR	D	L
A	0.562" +0.0 -0.002	15.0"
B	0.587" +0.0 -0.002	14.5"

Figure 3 Pumpout Tube Detail

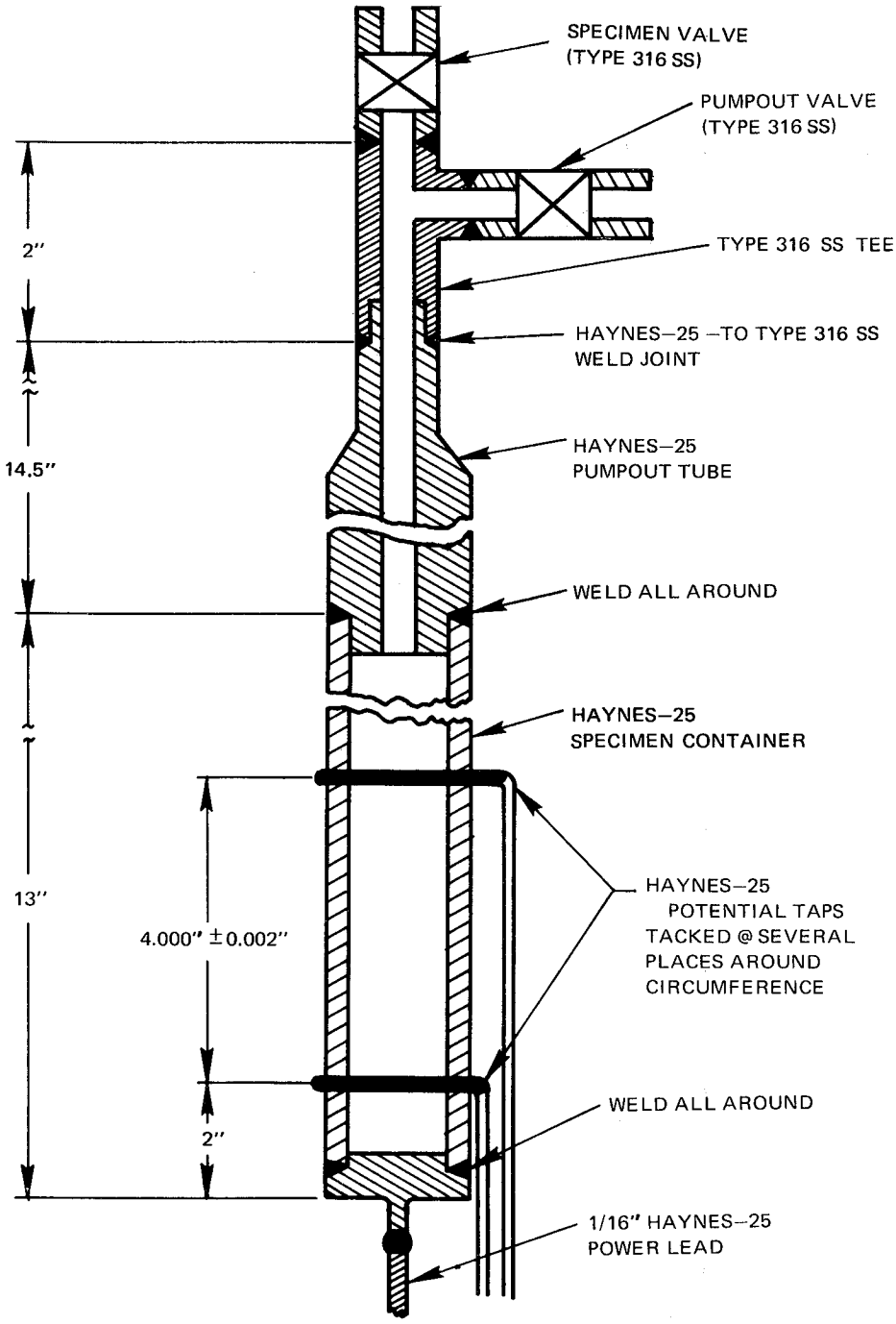

Figure 4 Specimen Assembly for Specimen Container Calibration and Lithium Resistivity Measurements

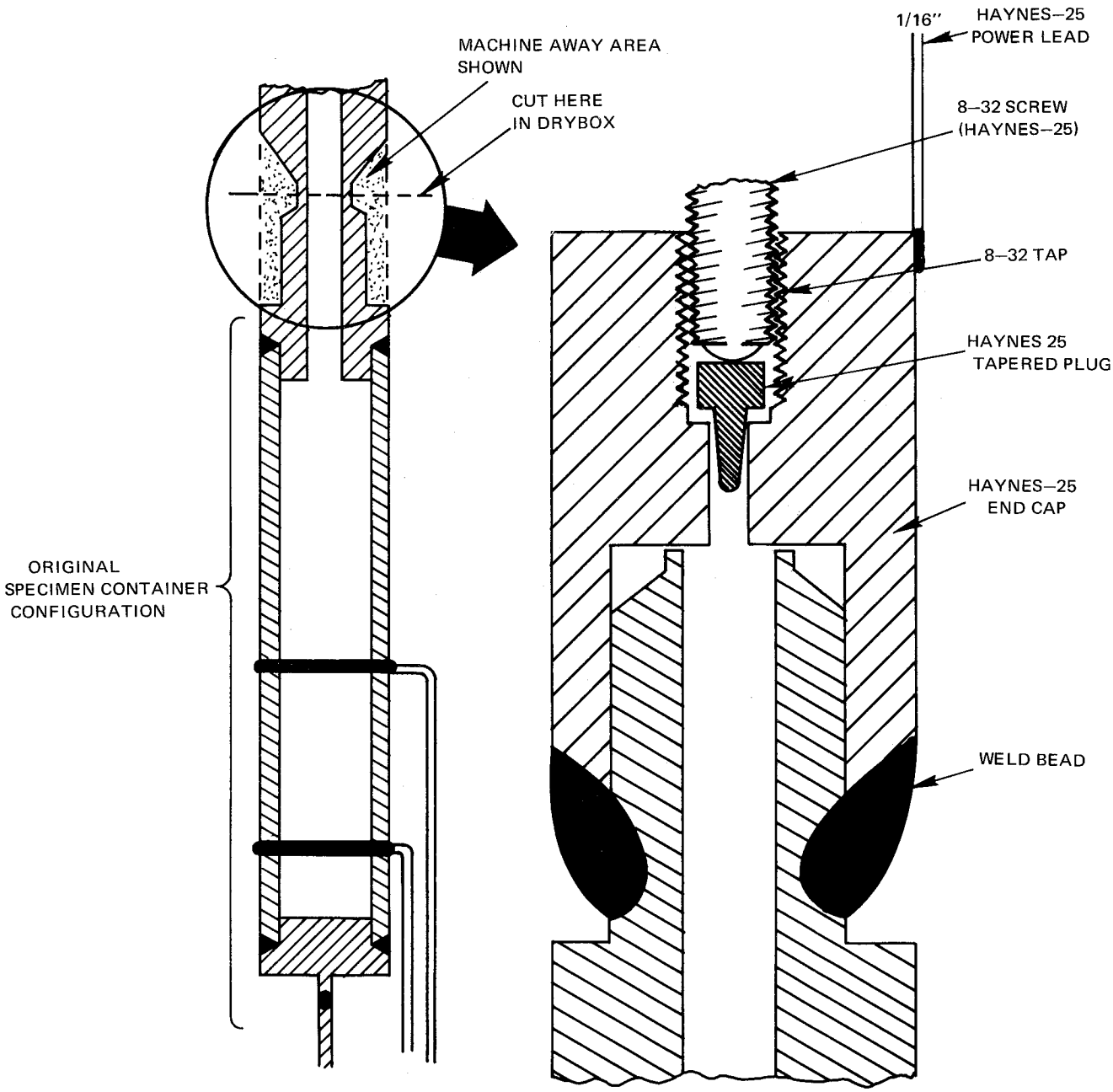

Figure 5 Redesigned Specimen Container for Lithium-Cesium Resistivity Measurements

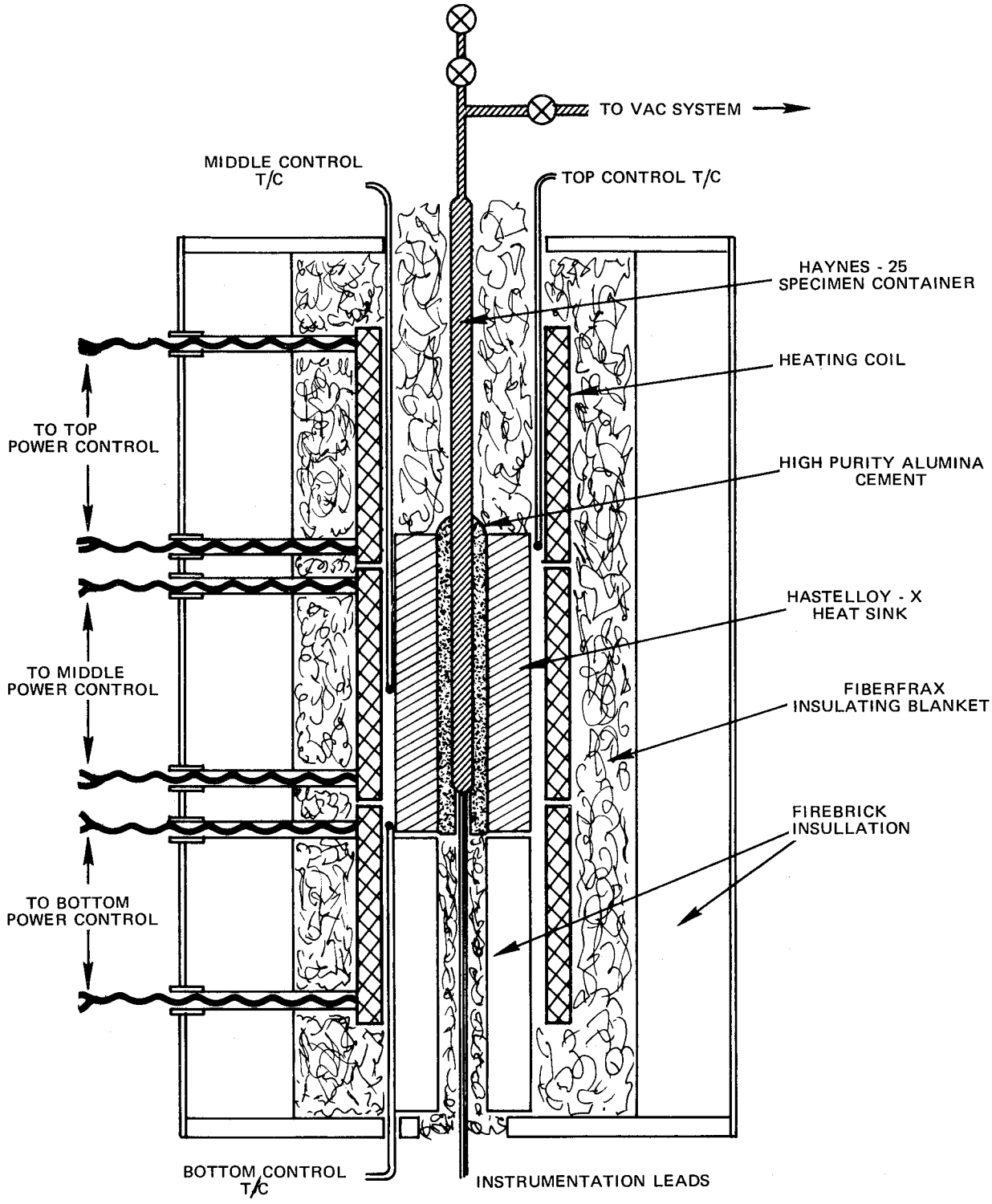

Figure 6 Heating System Schematic

The specimen container was cemented in a Hastelloy-X heat sink 2½-inches inside diameter by 4-inches outside diameter by 15-inches long. Figure 7 shows the specimen container in the heat sink. The heat sink was then centrally located in the heat zone. Three Pt/Pt-13% Rh thermocouples located between the inside diameter of the furnace core and the outside diameter of the heat sink were used to independently control the temperature of each zone of the furnace. The electric power to each zone was also independently controlled by powerstats, thus providing the flexibility required to maintain a uniform temperature along the specimen.

C. External Measuring System

The schematic diagram of the external measuring system is shown in Figure 8. All instrumentation leads were wired to a multiposition Lewis switch, the output of which was connected to the input of the potentiometer. This permitted a sequence of measurements to be made without disconnecting any of the wiring. The potentiometer used was a Leeds & Northrup Type K-2, calibrated to read accurately within ±0.7 microvolt. An Eppley standard cell calibrated to within ±1 microvolt was used to furnish the standardizing potential. The bucking voltage was supplied by a Leeds & Northrup constant voltage supply with a nominal output of 3 volts dc, a temperature coefficient of ±0.0005 percent/°C and a voltage regulation of ±0.0005 percent. The null indicator was a Leeds & Northrup guarded dc null detector having a sensitivity of 0.67 microvolt per division.

Specimen temperatures were determined using Pt/Pt-10% Rh thermocouples welded directly to the specimen container. The reference junctions were maintained at 0°C in an ice-water bath. Figure 9 shows the specimen container after the thermocouples and the potential taps had been welded in place.

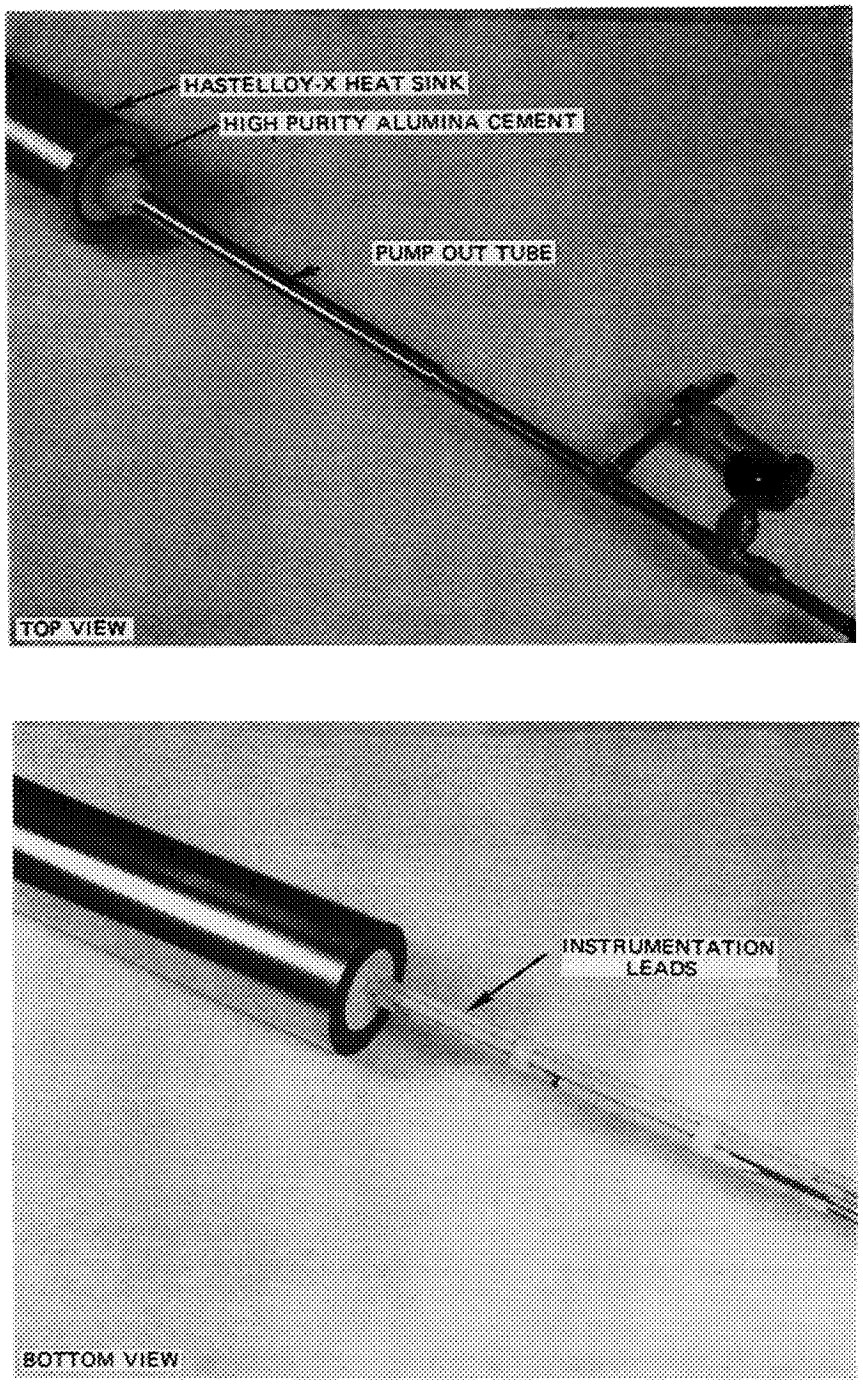

Figure 7 Top and Bottom Views of Specimen Container in Hastelloy-X Heat Sink

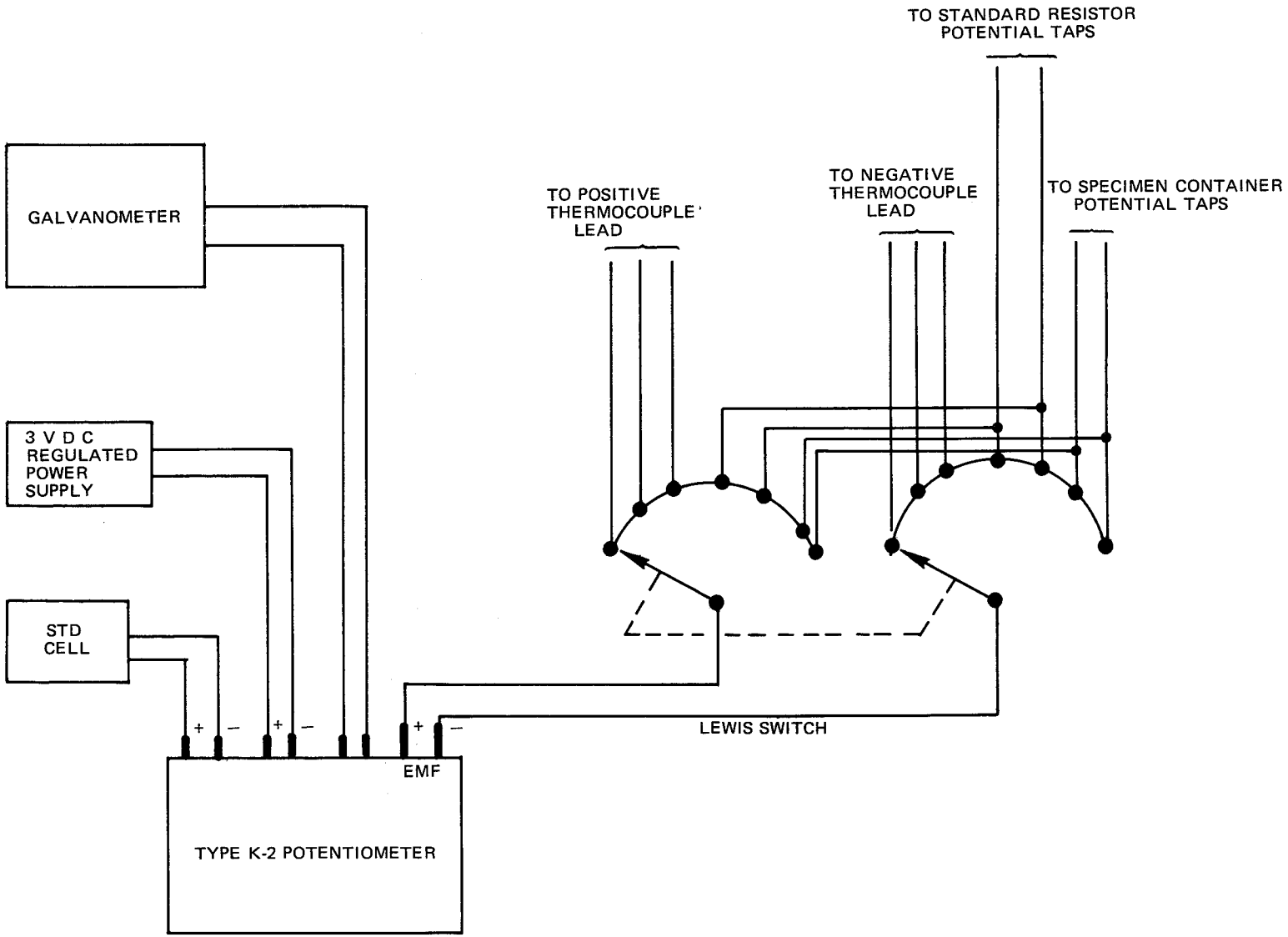

Figure 8 Schematic of External Measuring System

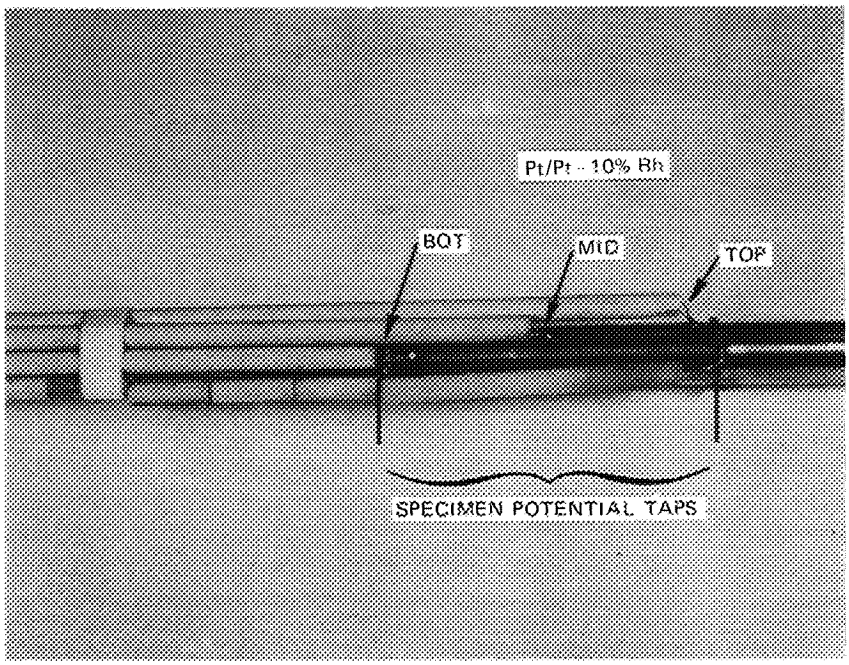

Figure 9 View of Specimen Container B Before Test Showing Location of Thermocouples and Potential Taps

V. EXPERIMENTAL PROCEDURES

A. Specimen Container Calibration

The resistance of the specimen container in parallel with the liquid metal column must be accurately known to obtain accurate values of the liquid metal resistance from equation (2). This resistance was measured for specimen container A as a function of temperature. The experimental configuration used was that shown in Figure 4.

Before any measurements were taken, the tube was mounted in the heat sink in the furnace, pumped and flushed several times with high purity argon, and evacuated to a pressure of less than 10^{-3} torr. In addition, the specimen was preoxidized by allowing it to soak overnight at a temperature of about 900°C. Then, a series of resistance measurements were made up to a temperature of 1068°C. The furnace was shut down and a second series of resistance measurements were made in the same temperature range. Both series of measurements were in agreement, indicating that the specimen container resistance did not change with time.

The resistance data for specimen container A is shown in Table I.

TABLE I

RESISTANCE OF HAYNES-25 SPECIMEN CONTAINER A

First Heating Cycle		Second Heating Cycle	
Temp (°C)	R (μ-ohms)	Temp (°C)	R (μ-ohms)
302 ± 1.1	887	384 ± 0.3	899
428 ± 0.8	907	486 ± 1.1	914
478 ± 0.7	914	590 ± 0.4	920
479 ± 0.4	912	658 ± 0.2	918
539 ± 1.0	920	865 ± 0.2	917
596 ± 0.5	920	975 ± 0.6	903
657 ± 0.5	924	1044 ± 0.3	893
710 ± 0.3	918		
766 ± 0.5	920		
870 ± 0.2	915		
980 ± 0.8	904		
1068 ± 0.4	894		

A least squares analysis of the data in Table I yielded the following equation for the resistance of specimen container A in the temperature range between 300°C and 1100°C:

$$R_A = 819.0 + 0.2792t - 2.160 \times 10^{-4} t^2 \quad (5)$$

where R_A = resistance of specimen container A ($\mu\Omega$)

t = temperature (°C)

The resistance of specimen container B can readily be obtained from the resistance of container A using the definition of resistivity:

$$\rho_A = \rho_B = R_A \frac{A_A}{L_A} = R_B \frac{A_B}{L_B} \quad (6)$$

where the subscripts A and B refer to specimen containers A and B, respectively, and the other symbols have been defined previously.

Since both specimen containers were machined from the same piece of bar stock, the assumption that their resistivities are the same is valid. Then, since the value for L, the distance between the potential taps, and the thermal expansion correction is the same for both specimen containers, we have for the resistance of specimen container B:

$$R_B = R_A \frac{A_A}{A_B} = R_A \frac{(Do^2 - Di^2)_A}{(Do^2 - Di^2)_B} \quad (7)$$

where

Do = Outside diameter of the specimen container
Di = Inside diameter of the specimen container
The subscripts A and B refer to specimen containers A and B, respectively

Specimen container A was used initially for the resistivity measurements. However, the specimen container had failed due to excessive oxidation when the thermocouples were tacked in place. Therefore, specimen container B had to be used to complete the program. The resistance of specimen container B, obtained from equations (5) and (7) for the temperature range between 300°C and 1100°C is given by:

$$R_B = 1009 + 0.3643t - 2.648 \times 10^{-4} t^2 \quad (8)$$

where R_B = resistance of specimen container B($\mu\Omega$)

t = temperature (°C)

Equation (8) was used to obtain the specimen container resistance R_C used in equation (2) to determine the liquid metal resistance.

B. Thermal Expansion Correction

The correction to the liquid metal resistivity due to thermal expansion of the Haynes-25 specimen container has been given by equation (4). The values for α at various temperatures are listed in Table II (Reference 7). These values were plotted as a function of temperature and the correction factors for each experimental point were obtained from the plot.

TABLE II

MEAN COEFFICIENT OF THERMAL EXPANSION FOR HAYNES-25 ALLOY

Temperature (°C)	Mean Coefficient of Thermal Expansion (1/°C)
21 - 93	12.3×10^{-6}
21 - 204	12.9×10^{-6}
21 - 316	13.5×10^{-6}
21 - 427	13.9×10^{-6}
21 - 538	14.4×10^{-6}
21 - 649	14.8×10^{-6}
21 - 760	15.4×10^{-6}
21 - 871	16.2×10^{-6}
21 - 982	16.9×10^{-6}
21 - 1093	17.7×10^{-6}

C. Lithium Resistivity Measurements

Prior to being placed in the inert atmosphere drybox, the specimen container and pumpout tube were cleaned ultrasonically in a bath of perchloroethylene, rinsed in reagent grade acetone and dried in a stream of argon. The lithium, the capsule parts, and all necessary equipment to complete fabrication of the experiment were introduced into the drybox and the system pumped for several days while maintaining a pressure below 10^{-4} torr. The box was pumped and flushed several times with high purity argon before any operations were started.

Before proceeding with the loading operation, the half inch diamter lithium sticks were scraped with a stainless steel knife, and two one gram samples taken for nitrogen analysis. When the analysis was complete, about 15 grams of lithium was introduced into the specimen container and the closure weld made in accordance with the scheme shown in Figure 4.

The vendor-furnished lithium analysis (Lithium Corporation of America) yielded the following results:

Element	Concentration (ppm)
Na	80
Fe	30
Ca	600
Si	80
Heavy Metals	30
Cl	40
N	150

The micro-Kjeldahl analysis of the two one gram lithium samples taken just prior to loading yielded 85 and 95 ppm nitrogen, in reasonally good agreement with the results obtained by Lithium Corporation.

After the capsule was filled, all thermocouples, potential taps, and power leads were tacked to the specimen container in the inert atmosphere drybox. This was necessary to eliminate the high oxygen contamination that would have resulted in the specimen container if these operations were performed in air. The specimen container was then helium leak tested, cemented in the heat sink with high purity alumina cement, installed in the furnace, pumped to less than 10^{-3} torr, flushed with high purity argon, and finally evacuated and sealed.

The following sequence of operations were performed in obtaining each data point:

1. Set the control thermocouples at the desired temperature and allow the furnace to stabilize at temperature;

2. Record specimen thermocouple readings and adjust furnace controls as required to maintain a maximum variation between the highest and lowest thermocouples of 2°C for at least one half hour;

3. Set the specimen current at about 0.3 – 0.4 ampere;

4. Record the potential drops across the standard resistor and the specimen in the forward direction;

5. Reverse the current and record the potential drops across the standard resistor and the specimen; and

6. Switch current to the forward direction and record the potential drop across the standard resistor. If this potential drop differs by more than 2 microvolts from that obtained for the standard resistor in step 4, the sequence is repeated.

D. Lithium-Cesium Resistivity Measurements

When the lithium resistivity measurements were completed, the specimen container was carefully removed from the heat sink and the pumpout tube was machined as indicated in Figure 5. Great care was taken to insure that the lithium was not exposed to air during this operation. The specimen container was then installed in the drybox and, when the box had been pumped and flushed several times with high purity argon, the pumpout tube was cut away from the specimen container at the point shown in Figure 5 and discarded. About five grams of cesium was poured through the resulting opening. The amount of cesium used was at least a twofold excess of that required for a saturated solution of cesium in lithium at 1100°C. The cesium was purchased from Electronic Space Products, Inc. to the following specification:

Element	Max. Concentration (ppm)
Cs	Balance
Na	300
K	100
Rb	300
Ca	100
Cl	20
Fe, Ni, Cr	200
N	100
All others	200

When the cesium had been placed in the specimen container, the redesigned end cap was fitted in place as shown in the right hand insert of Figure 5 and welded. The technique for evacuating and sealing the lithium-cesium specimen container may be explained with the aid of Figure 10. Prior to exposing any liquid metal to the drybox atmosphere, the 8-32 Haynes-25 screw was inserted and set in a half inch stainless steel rod and then slipped through a half inch swagelok fitting welded to the top of the box. A greased "O" ring formed a pressure/vacuum seal between the rod and the swagelok fitting. A metal tube was slipped over the assembly and fixed in place with sealing wax. This permitted the swagelok fitting to be bathed in argon, which prevented air leakage into the box in the event of slight leakage past the "O" ring. Then, after the top end cap was welded in place the specimen container was clamped in the vise and aligned so that the Haynes-25 screw was concentric with the corresponding tapped hole in the end cap. The vise was then strapped to the bottom of the box. The Haynes-25 screw was positioned about 1/8-inch from the top of the end cap and the box was evacuated. The pressure in the box was maintained below about 10^{-4} torr for several hours, after which the Haynes-25 screw was tightened in place forcing the tapered plug into its mating hole. This formed an effective vacuum seal inside the specimen container. (This sealing technique was helium leak tested successfully prior to attempting it with the specimen container). When the specimen container was sealed, the box was back-filled with high purity argon and the final closure was made by welding the Haynes-25 screw to the end cap. The specimen container was leak tested by immersing it in liquid nitrogen until thermal equillibrium was reached, followed by immersion in room temperature perchlorethylene while looking for gas bubbling. The absence of gas bubbles indicated that the specimen container was leak tight.

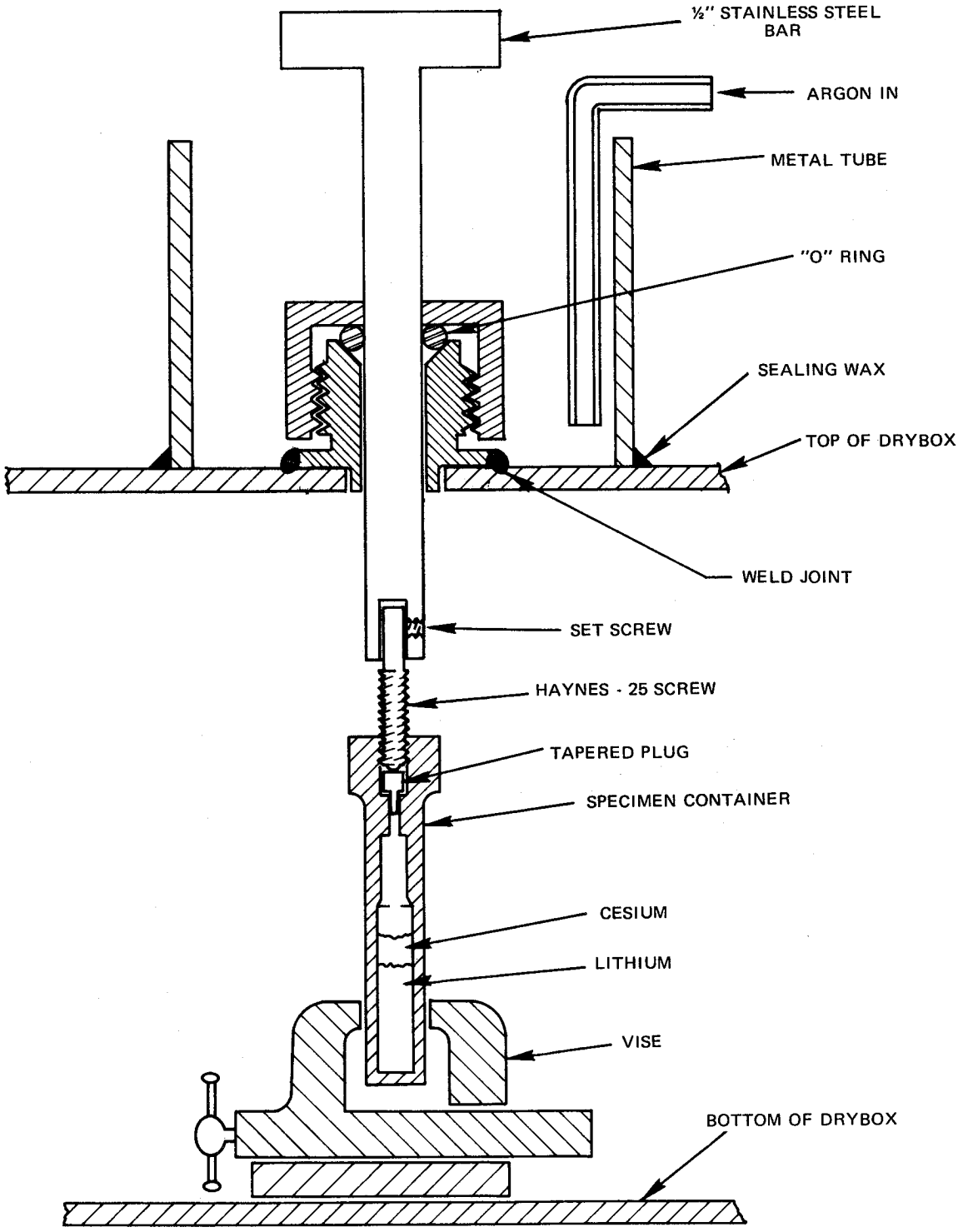

Figure 10 Schematic of Technique for Sealing Lithium-Cesium Capsule

Thermocouples, potential taps, and power leads were then tacked in place. The specimen container was cemented in the heat sink and installed in the furnace. The procedure for making lithium-cesium resistivity measurements was the same as that for the lithium, with the exception that the lithium-cesium measurements were made as a function of time until the values remained constant for at least one hour. This was to insure that the lithium was indeed saturated with cesium. Saturation was reached approximately one-half hour after a stable specimen temperature was achieved. Several checks were made by allowing the specimen to remain at temperature overnight. The overnight values agreed with previous ones within plus or minus a few tenths of a percent.

VI. RESULTS AND DISCUSSION

The results of the lithium resistivity measurements are shown in Table III, and the lithium-cesium results are presented in Table IV. The corresponding plots of resistivity versus temperature are shown in Figures 11 and 12, respectively. In order to check the reproducibility of the results, the data points were recorded in a number of heating cycles, in which the furnace was shut down and allowed to cool before the next series of measurements were obtained. Three heating cycles were used for the lithium data and four heating cycles for lithium-cesium. As the data in Tables III and IV and in Figures 11 and 12 indicate, the results were quite reproducible. The temperature error quoted in the tables represents the maximum difference between a given thermocuple reading and the average of all readings.

Least squares analysis of the data in Tables III and IV yielded the following equations for electrical resistivity:

- Lithium:

$$\rho_{Li} = 21.48 + 0.03170t - 5.913 \times 10^{-6} t^2 \quad (9)$$

- Lithium saturated with cesium

$$\rho_{Li\text{-}Cs} = 41.97 - 0.01585t + 2.271 \times 10^{-5} t^2$$

where ρ is the electrical resistivity in micro-ohm-cm and t is in °C. (10)

The effect of cesium saturation on the electrical conductivity of liquid lithium to 1100°C is small. This is graphically illustrated in Figure 13, where the electrical resistivities of liquid cesium (Reference 6), liquid lithium and liquid lithium saturated with cesium are shown as a function of temperature. The lithium and lithium-cesium curves remain parallel to nearly 900°C, indicating that the solubility of cesium in lithium is very low in this range. It appears that the cesium acts as an impurity atom. This is in qualitative agreement with the results of Tepper, et al, (Reference 5) who report the solubility of cesium in lithium to be 0.02 mole percent at 760°C, increasing to 0.1 mole percent at 900°C.

According to Matthiessen's rule, when the concentration of an impurity atom is low, the change in electrical resistivity due to this impurity atom is independent of temperature. This residual resistance is caused by the scattering of electron waves by the impurity atoms which disturb the periodicity of the conducting lattice. Figure 14 is a plot of the difference in electrical resistivity between lithium saturated with cesium and liquid lithium as a function of temperature, showing that Matthiessen's rule is obeyed. The residual resistivity due to cesium atom impurities is about 0.7 microhm-centimeter, and is reasonably constant to 850°C. The increase in electrical resistivity due to cesium is 2.8 microhm-centimeters at 1100°C, the maximum temperature of these experiments. The resulting loss in generator efficiency in the lithium-cesium, two-cycle MHD generator is 2-percent at 800°C, and 5-percent at 1100°C, if this loss is attributed solely to the decrease in electrical conductivity of lithium due to cesium solubility.

TABLE III

ELECTRICAL RESISTIVITY OF LIQUID LITHIUM

First Heating Cycle		Second Heating Cycle		Third Heating Cycle	
Temperature (°C)	$\rho(\mu\Omega$-cm)	Temperature (°C)	$\rho(\mu\Omega$-cm)	Temperature (°C)	$\rho(\mu\Omega$-cm)
364 ± 0.1	32.3	365 ± 0.7	32.0	668 ± 0.7	39.3
425 ± 0.4	34.1	512 ± 1.0	36.1	895 ± 0.3	45.0
577 ± 0.7	37.6	609 ± 0.2	39.4	973 ± 0.7	46.9
684 ± 0.6	40.6	807 ± 0.5	43.0		
747 ± 0.6	42.0				

TABLE IV

ELECTRICAL RESISTIVITY OF A SATURATED SOLUTION OF CESIUM IN LIQUID LITHIUM

First Heating Cycle		Second Heating Cycle	
Temperature (°C)	$\rho(\mu\Omega$-cm)	Temperature (°C)	$\rho(\mu\Omega$-cm)
769 ± 0.5	43.1	819 ± 0.5	44.2
824 ± 0.4	44.4	910 ± 0.1	46.2
874 ± 0.1	45.6	927 ± 0.5	46.5
930 ± 0.5	47.4	955 ± 0.5	47.6
		982 ± 0.5	48.1

Third Heating Cycle		Fourth Heating Cycle	
Temperature (°C)	$\rho(\mu\Omega$-cm)	Temperature (°C)	$\rho(\mu\Omega$-cm)
768 ± 0.5	43.1	777 ± 0.4	43.4
932 ± 0.6	46.9	845 ± 0.5	45.1
976 ± 0.6	48.1	963 ± 1.0	47.7
1002 ± 0.6	48.7	1042 ± 0.7	50.2
		1066 ± 1.0	50.9
		1086 ± 0.8	51.7
		1094 ± 0.9	51.8

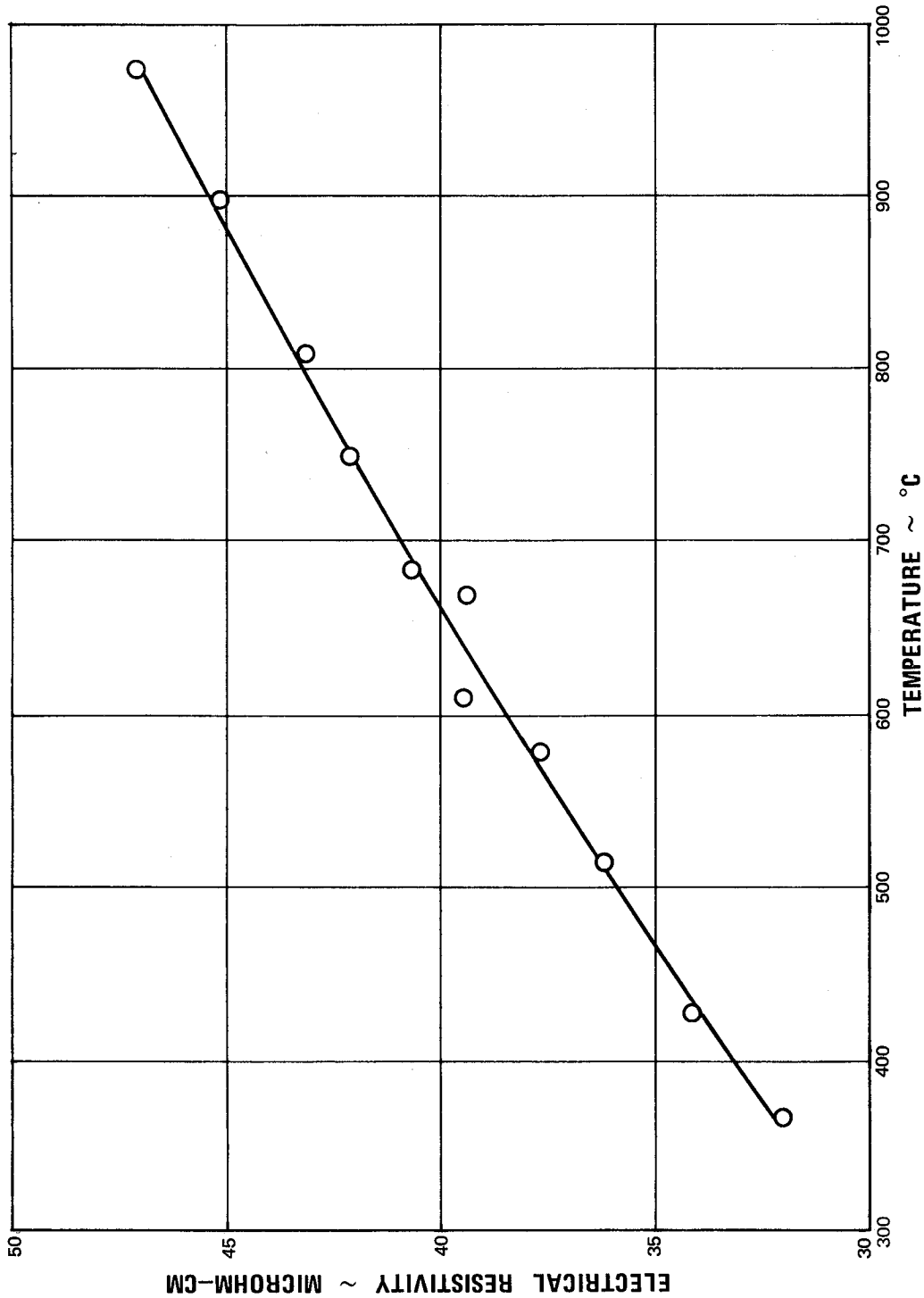

Figure 11 Electrical Resistivity of Lithium

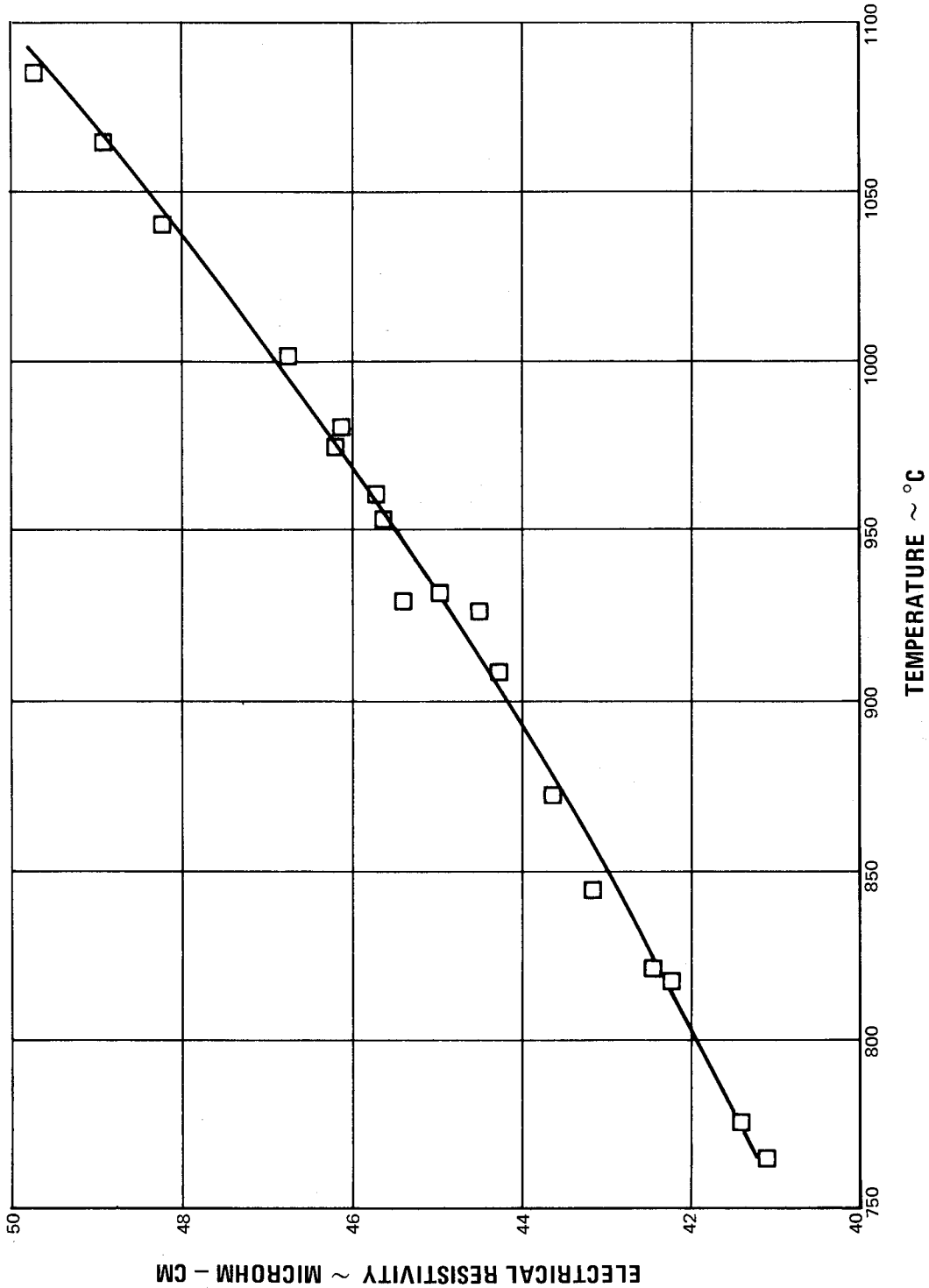

Figure 12 Electrical Resistivity of Cesium Saturated Liquid Lithium

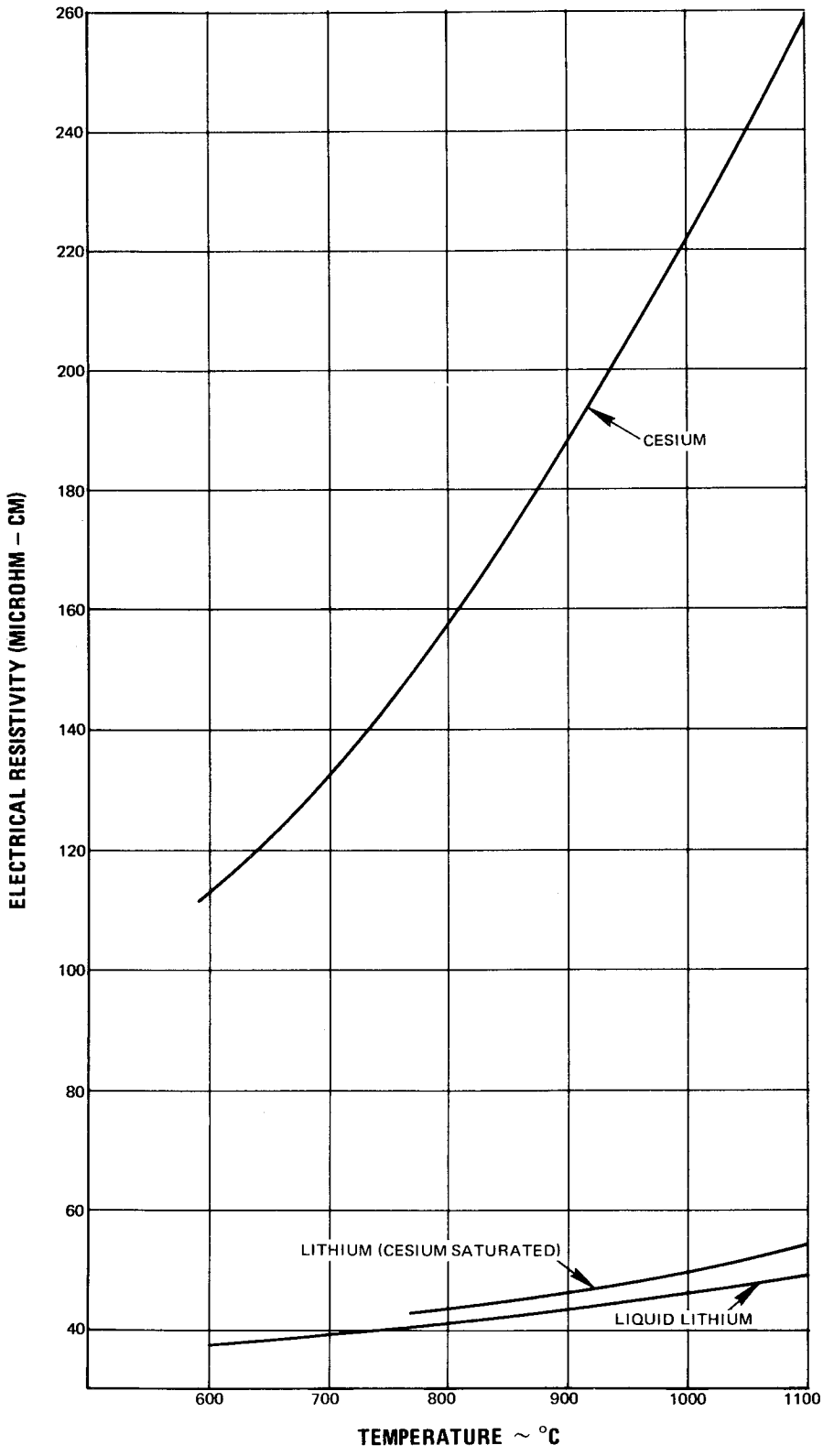

Figure 13 Effect of Cesium Solubility on the Electrical Resistivity of Liquid Lithium

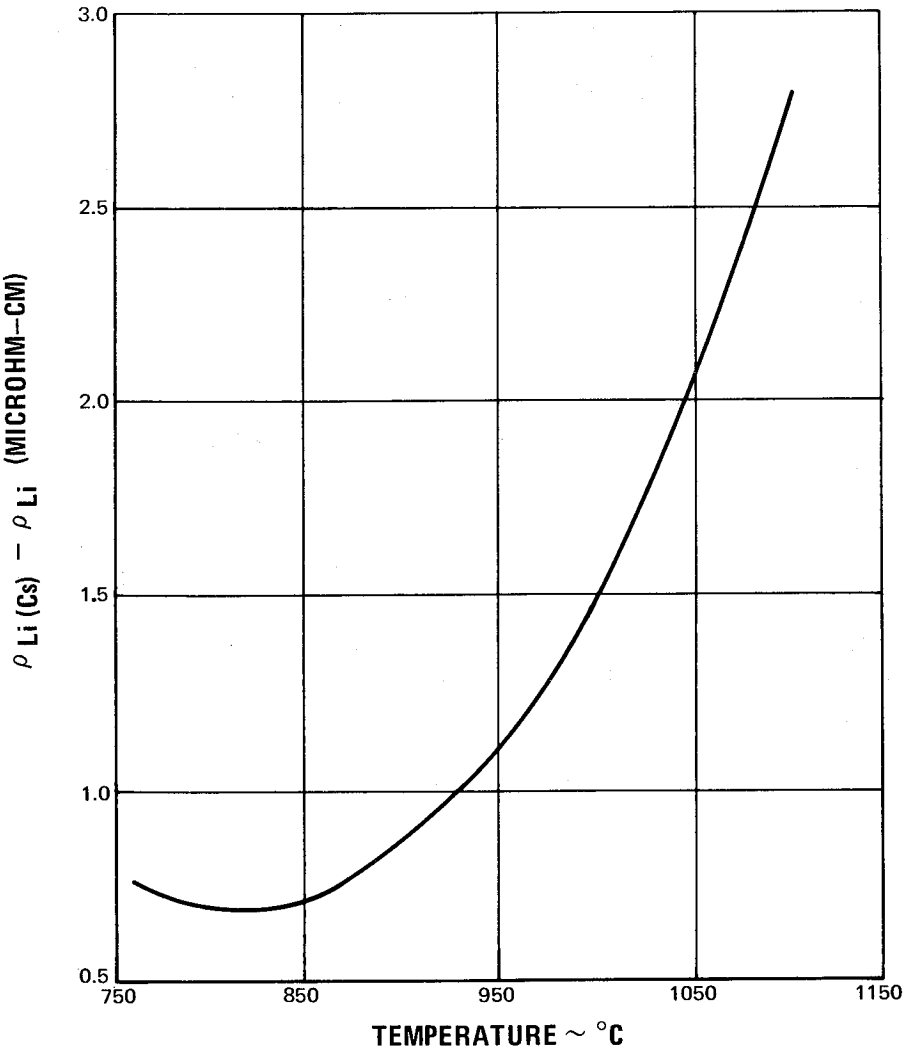

Figure 14 Electrical Resistivity Contribution of Cesium to Saturated Solutions of Cesium in Lithium

VII. REFERENCES

1. D. G. Elliot, D. J. Cerini, and E. Weinberg: Investigation of Liquid Metal MHD Power Conversion, AIAA Paper No. 64-760, presented at the Third Biennial Aerospace Power Systems Conference, Philadelphia, Pennsylvania, September 1-4, 1964.

2. D. G. Elliot, D. Cerini, L. Hays, E. Weinberg, and D. O'Connor: Liquid MHD Power Conversion, SPS 37-34, Vol. IV Jet Propulsion Laboratory, Pasadena, California, August 31, 1965, p. 163.

3. S. M. Kapelner: The Electrical Resistivity of Lithium and Sodium-Potassium Alloy, Pratt & Whitney Aircraft – CANEL Report PWAC-349, June 1961.

4. D. V. Rigney, S. M. Kapelner, and R. E. Cleary: The Electrical Resistivity of Lithium and Columbium -1 Zirconium Alloy to 1430°C, Pratt & Whitney Aircraft – CANEL Report TIM-854, September 1965.

5. F. Tepper, R. Udavcak, and J. Zelenak: Determination of the Solubility of Potassium and Cesium in Lithium, MSA Research Corporation, Report MSAR 64-19, April 1964.

6. S. M. Kapelner and W. D. Bratton: The Electrical Resistivity of Sodium, Potassium, Rubidium and Cesium in the Liquid State, Pratt & Whitney Aircraft – CANEL Report PWAC-376, June 1962.

7. Haynes-Stellite Corporation Product Bulletin

DISTRIBUTION LIST FOR FINAL REPORT

UNDER CONTRACT NAS7-658

1. Prof. B. A. Reese
   Jet Propulsion Center
   School of Mechanical Engineering
   Purdue University
   Lafayette, Indiana 47907

2. Mr. Robert English
   Lewis Research Center
   21000 Brookpark Road
   Cleveland, Ohio 44135

3. Mr. Simon V. Manson, RNP
   National Aeronautics and Space Administration
   Washington, D. C. 20546

4. Dr. George W. Sutton
   Avco Everett Research Laboratory
   2385 Revere Beach Parkway
   Everett, Massachusetts 02149

5. Dr. Morris A. Zipkin
   General Electric Company
   Building 701, Mail Zone N
   Cincinnati, Ohio 45215

6. Dr. George A. Brown
   Department of Mechanical Engineering
   Wales Hall
   University of Rhode Island
   Kingston, Rhode Island 02881

7. Mr. Larry Prem
   Atomics International Division
   P. O. Box 309
   Canoga Park, California 91305

8. Dr. Novak Zuber
   School of Mechanical Engineering
   Georgia Institute of Technology
   Atlanta, Georgia 30332

9. Mr. R. M. Bernero
   General Electric Company
   Isotope Power Systems Operation
   Space Division
   P. O. Box 8661
   Philadelphia, Pennsylvania 19101

10. Miss Ruth Weltmann
    Lewis Research Center
    21000 Brookpark Road
    Cleveland, Ohio 44135

11. Mr. R. W. Dickinson
    Liquid Metal Information Center
    P. O. Box 309
    Canoga Park, California 91305

12. Mr. James Lynch, RNP
    National Aeronautics and Space Administration
    Washington, D. C. 20546

13. Mr. William Woodward, RN
    National Aeronautics and Space Administration
    Washington, D. C. 20546

14. Dr. Fred Schulman, RNP
    National Aeronautics and Space Administration
    Washington, D. C. 20546

15. Mr. Jerome P. Mullin, RNT
    National Aeronautics and Space Administration
    Washington, D. C. 20546

16. Mr. Joseph W. Haughey, SV
    National Aeronautics and Space Administration
    Washington, D. C. 20546

17. Mr. Preston T. Maxwell, RNW
    National Aeronautics and Space Administration
    Washington, D. C. 20546

18. Dr. Hermann H. Kurzweg, RR
    National Aeronautics and Space Administration
    Washington, D. C. 20546

19. Mr. John A. Satkowski
Office of Naval Research
Power Program, Code 473
Washington, D. C. 20360

20. Dr. Edward S. Pierson
University of Illinois at Chicago Circle
P. O. Box 4348
Chicago, Illinois 60680

21. Dr. Michael Petrick
Argonne National Laboratory
Reactor Engineering Division
Building 11
Argonne, Illinois 60439

22. Dr. John Evvard
Lewis Research Center
21000 Brookpark Road
Cleveland, Ohio 44135

23. Dr. Frederick H. Morse
Department of Mechanical Engineering
University of Maryland
College Park, Maryland 20742

24. Dr. O. E. Dwyer
Brookhaven National Laboratory
Upton, New York 11973

25. Dr. Art Fraas
Oak Ridge National Laboratory
Oak Ridge, Tennessee 37830

26. Dr. M. Klein
U. S. Atomic Energy Commission
Division of Reactor Development
Washington, D. C. 20545

27. Dr. Robert Gordon
Aerojet General Corporation
Azusa, California 91702

Balance to Mr. George A. Mitchell
Mail Station 111-122
Jet Propulsion Laboratory
4800 Oak Grove Drive
Pasadena, California 91103